

UNCLASSIFIED

AD . 405 479

DEFENSE DOCUMENTATION CENTER

FOR

SCIENTIFIC AND TECHNICAL INFORMATION

CAMERON STATION, ALEXANDRIA, VIRGINIA



UNCLASSIFIED

NOTICE: When government or other drawings, specifications or other data are used for any purpose other than in connection with a definitely related government procurement operation, the U. S. Government thereby incurs no responsibility, nor any obligation whatsoever; and the fact that the Government may have formulated, furnished, or in any way supplied the said drawings, specifications, or other data is not to be regarded by implication or otherwise as in any manner licensing the holder or any other person or corporation, or conveying any rights or permission to manufacture, use or sell any patented invention that may in any way be related thereto.

63-35



ORA-63-3

ORA-63-3

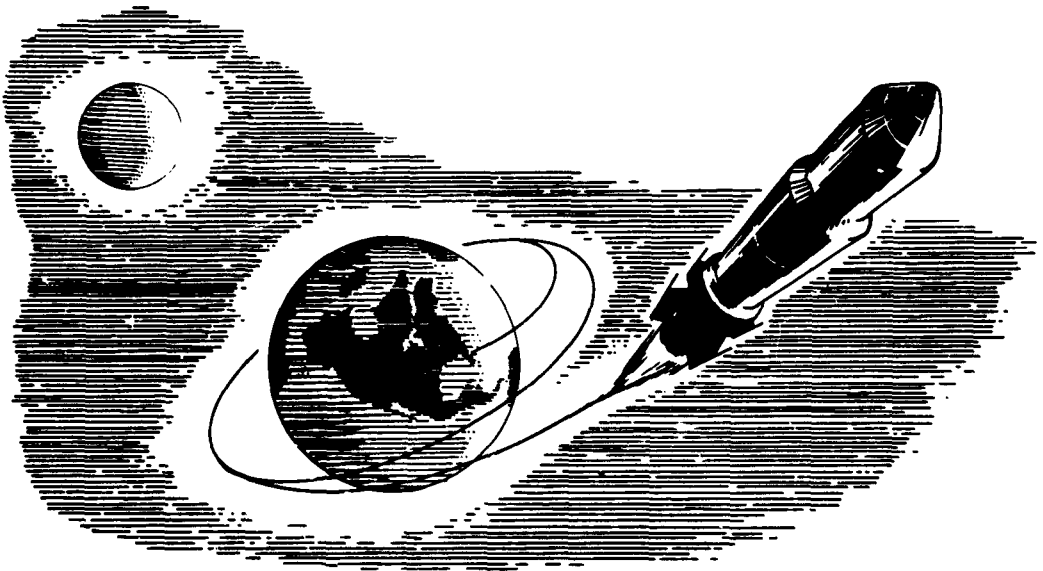
405479

HEADQUARTERS OFFICE OF AEROSPACE RESEARCH
TECHNICAL REPORT

Contract AF 29(600)-3020

STUDY OF A TRACER METHOD FOR SOLID PROPELLANTS

David Fleischer



OFFICE OF RESEARCH ANALYSES
HOLLoman AIR FORCE BASE
NEW MEXICO

February 1963

405 479

Qualified requesters may obtain copies of this report from the Armed Services Technical Information Agency (ASTIA). Orders will be expedited if placed through your librarian or other staff member designated to request and receive documents from ASTIA.

Copies of this report are for sale to the general public through the Office of Technical Services, Department of Commerce, Washington 25, D. C.

ORA-63-3

ORA-63-3

Contract AF 29(600)-3020

STUDY OF A TRACER METHOD FOR SOLID PROPELLANTS

David Fleischer

Reaction Motors Division
Thiokol Chemical Corporation

RMD Report 5502-F

Science and Engineering Division
Office of Research Analyses

OFFICE OF AEROSPACE RESEARCH
UNITED STATES AIR FORCE
Holloman Air Force Base, New Mexico

February 1963

FOREWORD

This is the final report under Contract AF29(600)-3020 and covers the period 19 June 1961 to 18 June 1962. It is preceded by two reports written under the following Contracts: AF29(600)-2422 (24 May 1960 - 20 May 1961), AF29(600)-2067 (20 June 1959 - 20 March 1960). The entirety of this series was under the cognizance of the Office of Research Analyses, Air Force Office of Aerospace Research, Holloman Air Force Base, New Mexico.

The following personnel have contributed to the present report: W. Stark, B. Hornstein, B. Dawson and W. Romaine.

We wish to acknowledge the continuing interest and support of Dr. Friedrich G. Penzig, our Technical Monitor, who originally conceived the method of determining solid engine burning rates by means of photoemissive deposits.

ABSTRACT

A photometric method for determining local burning rates in solid propellant motors is described. Metallic salt-polymer mixtures (tracers) are inserted in known locations in the motor. Resonant radiation from the vaporized metal provides light pulses in the motor exhaust. Spectrographic time resolution of these pulses and the known distances between deposits in the grain yield the burning rates. Preliminary strand experiments are used to estimate burning rates of tracer and propellant under engine conditions. These values are introduced in an expression relating accuracy of photometric burning rate to tracer thickness, separation between tracer deposits, and tracer and propellant burning rates. Tracer thickness and separation in the test engine for a desired accuracy are thus defined. Engine burning rates reproducible to ± 7 per cent for a one centimeter separation were easily obtained.

SUMMARY

This report describes the development of a photometric method for determining local burning rates in solid propellant engines. Metallic salt deposits are inserted at known locations in the grain. Vaporization of these deposits and subsequent thermal excitation of their resonant frequency provides light pulses in the motor exhaust. The spectrographic time resolution of these signals and their predetermined locations in the grain yield the burning rate.

The effects of different salt formulations ("tracers") and their mode of insertion were studied in strand burning experiments by comparing fuse-wire burning rates for pure and adulterated sections of propellant. It was found that if the depth of a tracer deposit was limited to 10 per cent of the total propellant distance between deposits there was no perturbation in the burning rate. The burning rate was not affected whether the tracer was in the form of a non-reactive salt, an oxidizing salt or as the oxidizing component of a propellant formulation. The accuracy of the method was established by comparing photometric burning rates with fuse-wire rates.

Tracer insertion techniques and instrumentation developed in the strand burning experiments were applied to an eighty pound thrust motor. The coolness of the expanded exhaust, in comparison to the strand burnt gases, necessitated an increase in the spectrograph slit width to raise the signal level. The resultant loss in spectral purity greatly decreased the signal-to-noise ratio, but the signal could still be readily discerned for a tracer area equal to 1 per cent of the total burning area. Tracers in the form of salts were satisfactory in the strand tests. In the high pressure motor environment the flame front flashed through the loose salt and ignited the walls of the tracer hole. The consequent spurious pressure rises, caused by the increased burning area, were eliminated by incorporating the photoemissive salt into a solid propellant mixture which was bonded to the hole in which it was deposited.

The above procedures yielded motor burning rates with an average reproducibility of 4 per cent for a 1 centimeter spacing between tracer deposits.

TABLE OF CONTENTS

	<u>Page</u>
INTRODUCTION	1
EQUIPMENT	3
Spectrometer	3
Signal Recorders	5
Strand Burner	5
Test Motor	8
Motor Grains	8
Propellant	12
Optical Path	12
TRACERS	16
STRAND EXPERIMENTS	17
Sample Preparation	17
Data Reduction	19
Signal Interpretation	20
Signal Duration	24
Temperature Effect	24
Effect of Tracer Deposits	27
Signal Intensity	30
Recommended Procedure	30

TABLE OF CONTENTS (Cont.)

	<u>Page</u>
MOTOR BURNING RATES	32
Tracer Insertion	32
Firing Procedure	33
Data Reduction	34
Spectrometer Aperture	36
Background Radiation	37
Signal Detection	39
Motor Pressure	40
Burning Rates	40
Discussion	43

LIST OF TABLES

<u>Table</u>		<u>Page</u>
I	COMPOSITION OF BF-122 MOD-1 PROPELLANT	13
II	CRAWFORD BOMB BURNING RATES FOR BF-122 MOD-I PROPELLANT	15
III	TRACER METHOD BURNING RATES	23
IV	COMPARISON OF TRACER AND FUSE WIRE BURNING RATES FOR THE SAME ENVIRONMENT	26
V	EFFECT OF CEMENTED INTERFACES ON THE BURNING RATE	28
VI	EFFECT OF LITHIUM PERCHLORATE ON THE BURNING RATE	29
VII	TRACER METHOD ENGINE BURNING RATES	41

LIST OF FIGURES

<u>Figure</u>		<u>Page</u>
1	INSTRUMENTATION FOR RECORDING SIGNAL FROM TRACER DEPOSITS	4
2	STRAND BURNER	6
3	FUSE-WIRE CIRCUIT FOR STRAND BURNER	7
4	EXPERIMENTAL ENGINE IN PROTECTIVE TUBE	9
5	IGNITION CIRCUIT FOR SOLID MOTOR	10
6	SLOTTED TUBE GRAIN WITH TRACER DEPOSITS	11
7	EXHAUST TEMPERATURE VERSUS CHAMBER PRESSURE FOR BF-122 MOD-I	14
8	CROSS SECTION OF FUSED STRAND WITH TRACER DEPOSITS	18
9	TYPICAL STRAND BURNING RECORD ON 35 MM FILM	21
10	MOTOR PRESSURE TRACE	35
11	RADIATION FROM MOTOR SQUIB	38
12	RADIATION FROM MOTOR GRAIN	38

INTRODUCTION

It is well known that solid propellant engines cannot be satisfactorily designed on the basis of strand burning rates determined in laboratory combustion bombs. In some cases, when the mass flow of burnt gas over the propellant surface is not too large, motor burning rates are smaller than those found in the laboratory. In other cases, if the burnt gas flow is sufficiently large, the rate is increased beyond that found in the static environment of the combustion bomb. In addition, burning rates are not simply a function of stream and propellant properties, but also depend upon the geometry of the surface. The practical result of these various effects is that several burning rates often obtain, in an unpredictable manner, in different locations of a solid motor at any given instant. In the past this design problem has been dealt with by such methods as visual examination of the burning surface after a difficult quenching operation and determination of burning rates by the insertion of fuse wires.

The purpose of the work described herein was to develop a photometric method for determining burning rates that held promise of being accurate and simple to apply. In the proposed method small deposits of metallic salts that are foreign to the propellant formulation were to be inserted in the motor at known locations. When the burning surface reached such a deposit the salt would be decomposed and discharged, in gaseous form, in the exhaust. This high temperature environment would stimulate emission of the characteristic resonant frequency of the metal component of the salt, and the light signals were to be detected spectroscopically. The time separation between signals and the spatial separation of the salt deposits would then yield a burning rate. Deposits in different locations could be distinguished by using a variety of metallic salts, each with its characteristic resonant frequency.

This method requires foreign inclusions in the solid propellant, and in order that the basic propellant characteristics not be modified the size of such deposits must be kept, individually and in sum, small. The feasibility, then, is dependent upon the spectrographic detection of very small concentrations of metallic species in combustion gases. The first contract year therefore was devoted to determining relationships between concentration and intensity of emitted

radiation in a variety of combustion gas environments¹. It was concluded that the following elements are suitable as tracer materials in both aluminized and non-aluminized propellants:

Lithium	Thallium
Indium	Manganese
Cesium	Lead
Rubidium	Gallium

During the second contract year attempts were made to apply this technique to the actual determination of rates in a solid propellant engine². Although tracers were detected, and much knowledge concerning instrumentation was gained, the results were ambiguous as far as burning rates were concerned. These negative results indicated that the step from laboratory work to field measurements on engines was premature.

The contract year whose results constitute the material of this report was divided into two phases. The first of these involved laboratory strand-burning experiments and was designed to provide a transition between previously acquired general knowledge on the detectability of tracers and the final application of this principle to the determination of burning rates in operational motors. Accordingly the strand experiments were concerned entirely with means of inserting tracer materials into the propellant, effects of tracer materials and the method of insertion on burning rates, and the interpretation of tracer signals in relation to events occurring in the propellant.

This information was applied to the second phase of the program in which the successful determination of rates in an operational engine was achieved.

-
1. W. Stark and H. G. Wolfhard "Study of A Tracer Method For Solid Propellants", Air Force Missile Development Center Tech. Note AFMDC-TN-60-10, Holloman Air Force Base, N. M. (1960).
 2. W. Stark and B. Hornstein "Study of A Tracer Method For Solid Propellants", Air Force Office of Scientific Research Tech. Rep. AFOSR/DRA-62-6, Directorate of Research Analyses, Holloman Air Force Base, N. M. (1962).

EQUIPMENT

The equipment arrangement for the strand-burning experiments and motor experiments are shown in Figure 1. The individual equipment items are described below.

Spectrometer

A Jarrell-Ash "Atomcounter" 1.5 meter grating instrument was used to detect the tracers in the propellant burnt gases. The sensing elements are photomultiplier tubes mounted behind the exit slits, and enough shielded cables were installed so that nine spectral lines could be detected at one time. Only three tubes, however, were used, in addition to one for the mercury line which was mounted at the factory and is only used for alignment purposes. These tubes were set at the following positions:

<u>Element</u>	<u>Spectral Line</u>	<u>RCA Tube</u>
Li	6708	6217
Ga	4172	IP28
Tl	5350	IP28

The 6217 PM tube offers higher sensitivity in the red, and is of the head-on type. No mount for this type was supplied by Jarrell-Ash, and one was constructed that had six adjustable degrees of freedom which permitted accurate alignment.

The voltage for the mercury tube was provided by a Jarrell-Ash power supply which also indicated tube output on a meter. This supply was found to have an unacceptably high noise level for the tracer work, and a Clegg Laboratories Model BL-RIA regulated supply was used to provide 1000 volts to the other tubes. The outputs from these tubes were displayed on an oscilloscope.

The general location of each exit slit was found by calculation. Final location was then made by illuminating the spectrometer with the desired frequency for each tube and peaking their outputs by fine adjustment of the exit slit. The thallium radiation was provided by a No. 50063 Osram lamp obtained from the Edmund Scientific Company, Barrington, New Jersey. The lithium and gallium light sources were improvised by soaking carbon rods in aqueous salt solutions and fixing them in the flame of an oxygen-hydrogen torch. Before these final adjustments in tube location were made the spectrometer

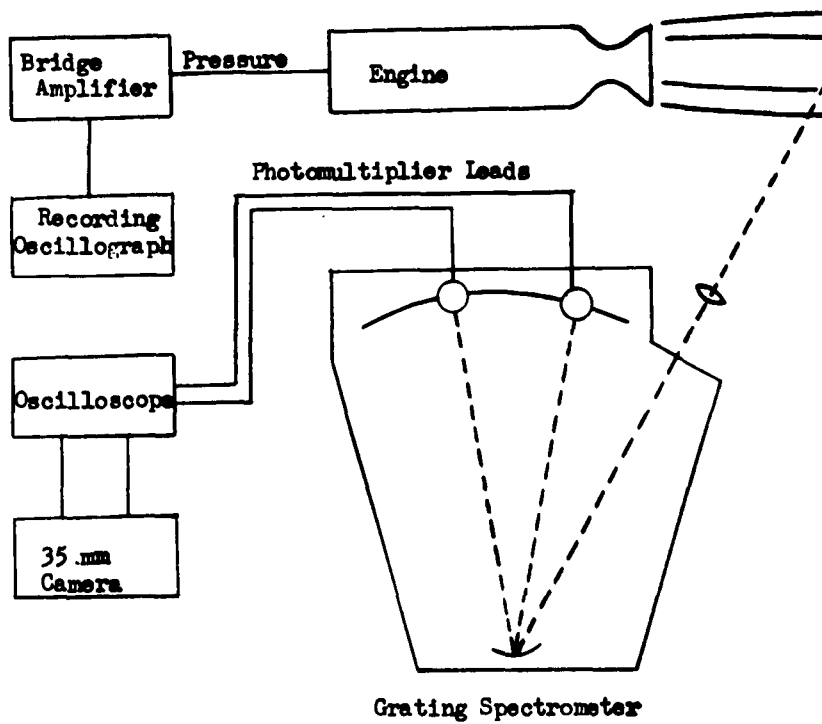


Figure 1. INSTRUMENTATION FOR RECORDING SIGNAL FROM TRACER DEPOSITS

was peaked on the mercury line with a mercury lamp and quartz refractor plate which were integral with the instrument. Thus, each tube was located relative to the mercury tube for its position of maximum output. By this device the spectrometer could be adjusted before each use for maximum output at all wavelengths by simply rotating the refractor plate to the position which was optimal for the mercury line.

The spectrometer was supplied with a fixed 25 micron entrance slit and 100 micron exit slits. These were used for all of the strand-burning experiments. When the detection of tracers in the exhaust of a motor was attempted it was found that these apertures were too small. A 100 micron entrance slit whose jaws were constructed from Schick razor blades was installed, and the exit slits were removed entirely. This arrangement was used for the motor burning rates.

Signal Recorders

The outputs from the tracer photomultiplier tubes were usually fed into a DuMont Type 322-A dual-beam oscilloscope that was equipped with a Fairchild Type 314A 35 mm movie camera. The film transport rate was regulated by a Type 314A electronic control of the same make. To record tracer signals with this camera the scope sweep was turned off, the time axis being generated by the moving film strip. The film used was Eastman Tri-X Type 5233.

For some purposes a single, differential signal input from two photomultiplier tubes was desired. In these cases a Tektronix Type 551-dual-beam oscilloscope with a Type D differential preamplifier was used. The Fairchild camera was also used to record data with this scope.

Motor pressure was sensed with a Teledyne transducer whose output was balanced and amplified with a 20 kilocycle Carrier amplifier. The motor pressure-versus-time curve was recorded with a CEC Type 1-124 recording oscillograph.

Strand Burner

The holder which was used to fix propellant strands in the vertical plane of the spectrograph's optical axis is shown in Figure 2. The double array of binding posts fixed to the Transite board served as terminals for timing wires which passed through the strand.

When the burning surface severed these fuse wires an electrical signal, generated by the circuit shown in Figure 3, was recorded by the oscilloscope.

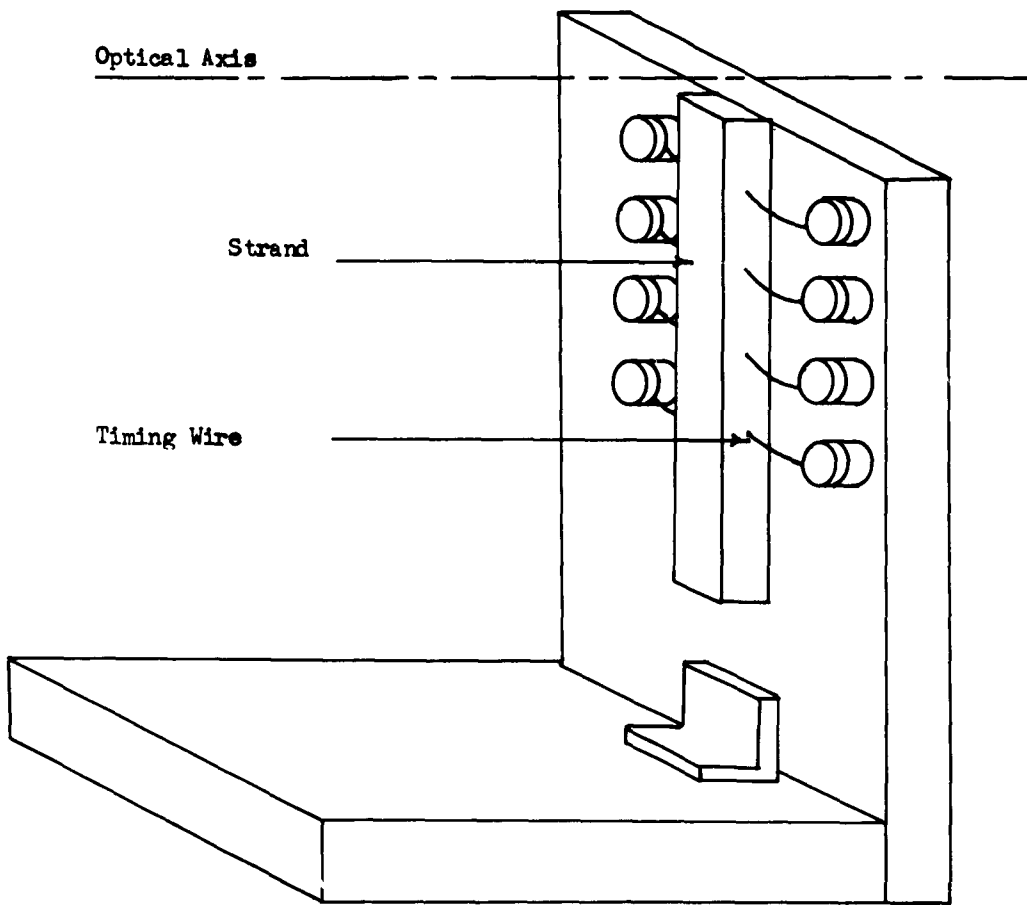


Figure 2. STRAND BURNER

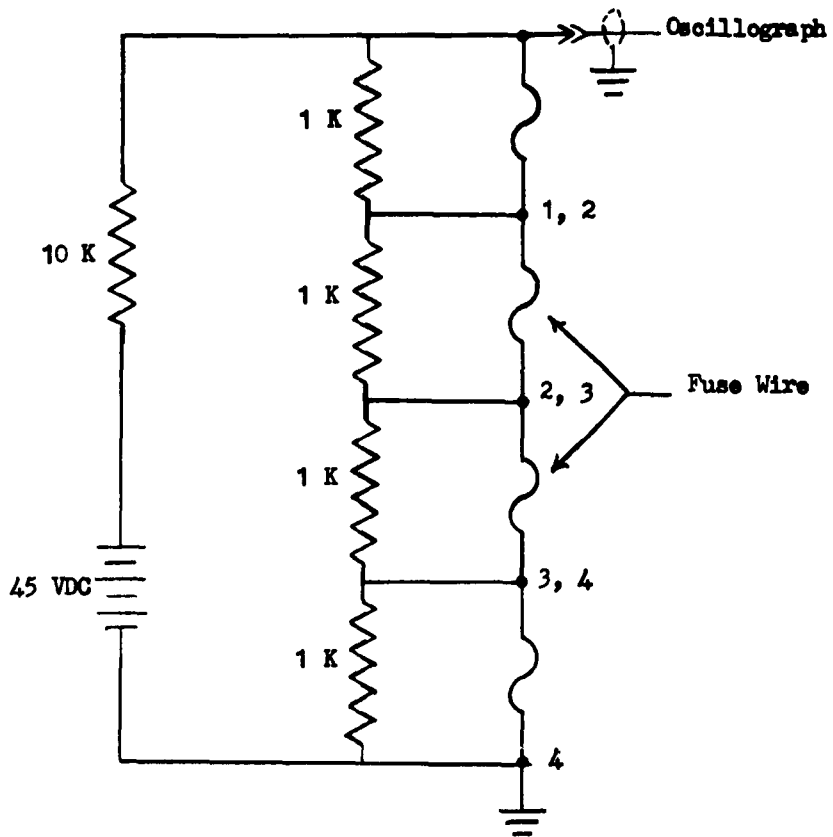


Figure 3. FUSE-WIRE CIRCUIT FOR STRAND BURNER

Test Motor

The engine that was used to determine burning rates is an uncooled "work-horse" design of three parts. The nozzle, made of copper with a throat diameter of 0.64 inch and an expansion ratio of 2.55, is sealed into the motor tube with an O-ring and secured with a snap ring. The head-end part has a pressure tap and blow-out disc, and is secured in the same fashion. The motor tube is fastened by a split-ring clamp inside of a protective pipe which, in turn, was bolted to an angle iron mount. The protective pipe has a rectangular opening at the motor nozzle exit plane through which the exhaust was examined.

The motor in operation inside its protective pipe is shown in Figure 4. The motor firing circuit is shown in Figure 5. The motor was fired in a concrete pit fitted with a hood and exhaust fan which discharged the combustion gases outside of the building. Exhaust scavenging was improved by a stove-pipe injection duct of somewhat smaller diameter than the protective pipe. The intake was located a few inches from this pipe, and the duct discharged into the exhaust fan.

Motor Grains

The motor grain, shown in Figure 6, is a slotted-tube type. This design³ combines progressive and regressive sections. The tubulated portion, which burns only internally, continuously increases its area. The slotted portion burns both internally and also from the exposed end surface, and continuously decreases its area. The relative proportions of these sections are so chosen that a flat motor pressure characteristic is achieved.

A neutrally burning grain was advantageous for these studies in that no variation in burning rate with pressure had to be accounted for. Thus, interpretation of the results for this preliminary work was simplified. Another advantage is that neutral character is had with only an internally burning surface. This gives maximum burning time for a given web thickness, and a small, economical motor could be used.

-
3. M. W. Stone, "The Slotted-Tube Grain Design", Rohm and Haas Co., Redstone Arsenal Res. Division, Huntsville, Ala., Report No. S-27, Dec. 1960.



5502-1

Figure 4. EXPERIMENTAL ENGINE IN PROTECTIVE TUBE

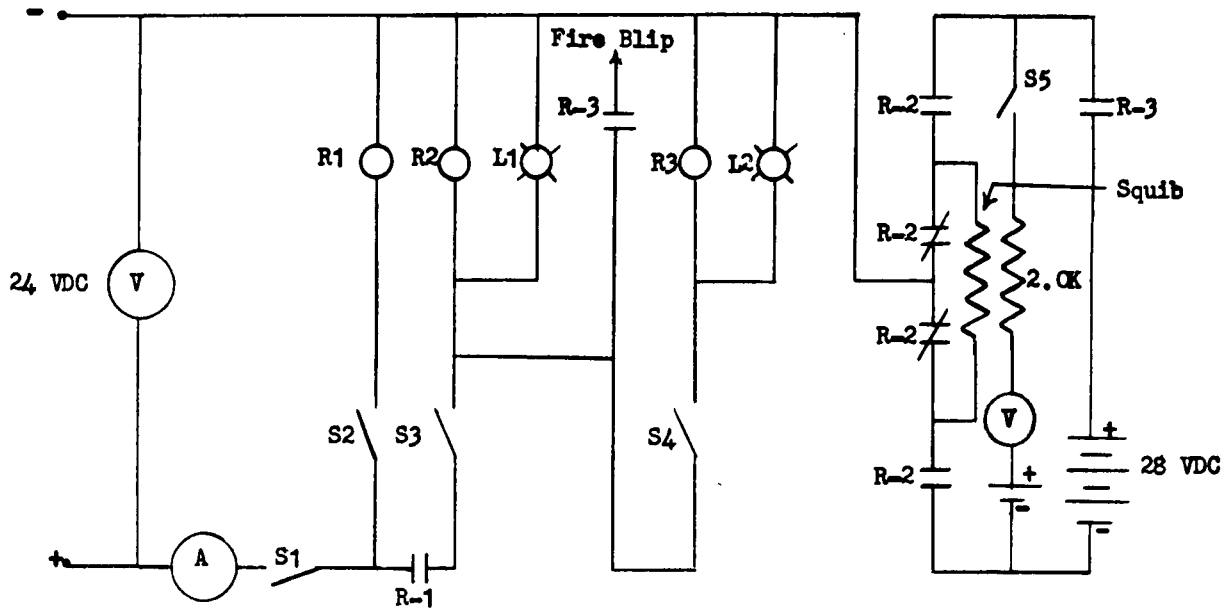


Figure 5. IGNITION CIRCUIT FOR SOLID MOTOR

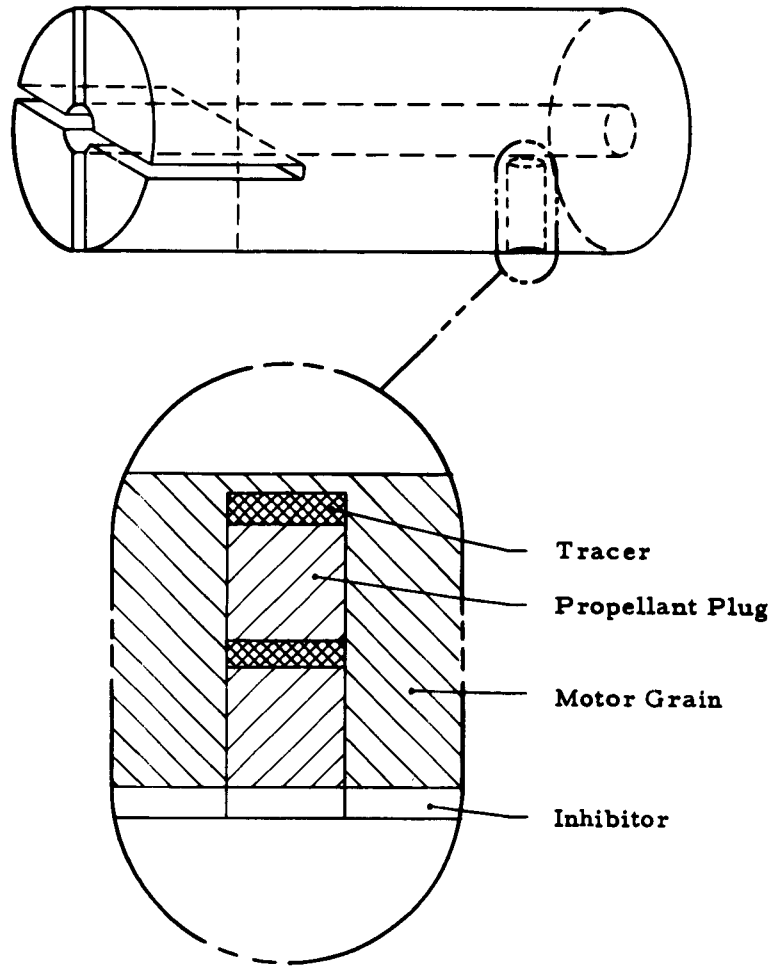


Figure 6. SLOTTED TUBE GRAIN WITH TRACER DEPOSITS

Propellant

The propellant that was used for both the strand-burning work and motor tests was BF-122 Mod I. This is a Class B, non-detonable substance according to I.C.C. regulations. The composition of this propellant is given in Table I. Propellant combustion calculations were performed by the computer group of Thiokol Chemical Corporation, Elkton Division, Elkton, Md., and the pertinent results, exhaust temperature for perfect expansion versus chamber pressure are plotted in Figure 7. Burning rates for several pressures, as determined in a Crawford bomb, are given in Table II.

Optical Path

Light from the rectangular aperture in the protective pipe was collected by a 4 x 5 inch front surface mirror which was over this opening and at a 45 degree angle to the vertical. This light was focused on the spectrometer entrance slit by means of an 11 cm diameter, 61 cm focal length Aero-Ektar lens having an f-number of six.

It was necessary to protect all exposed optics from the 20 per cent hydrogen chloride, and other corrosives, in the propellant combustion gases. The mirror and lens were boxed, and the light path from the box to the spectrometer was contained in a stove-pipe duct. This enclosure was made reasonably tight, excepting the opening in the bottom of the box through which exhaust radiation was admitted, and a slight positive pressure of nitrogen was maintained during all engine firings.

TABLE I

COMPOSITION OF BF-122 MOD-I PROPELLANT

<u>Ingredient</u>	<u>Weight Per cent</u>
AP* (Special Coarse)	57.40
AP (Fine Ground)	24.60
LP - 205**	11.51
LP - 33**	5.00
Paraquinone Dioxime	1.12
Sulfur	0.08
Benzyl mercaptan	0.04
Magnesium oxide	0.25

* Ammonium perchlorate

** These are liquid polysulfide polymers obtained from Thiokol Chemical Corporation, 780 N. Clinton Ave., Trenton, New Jersey

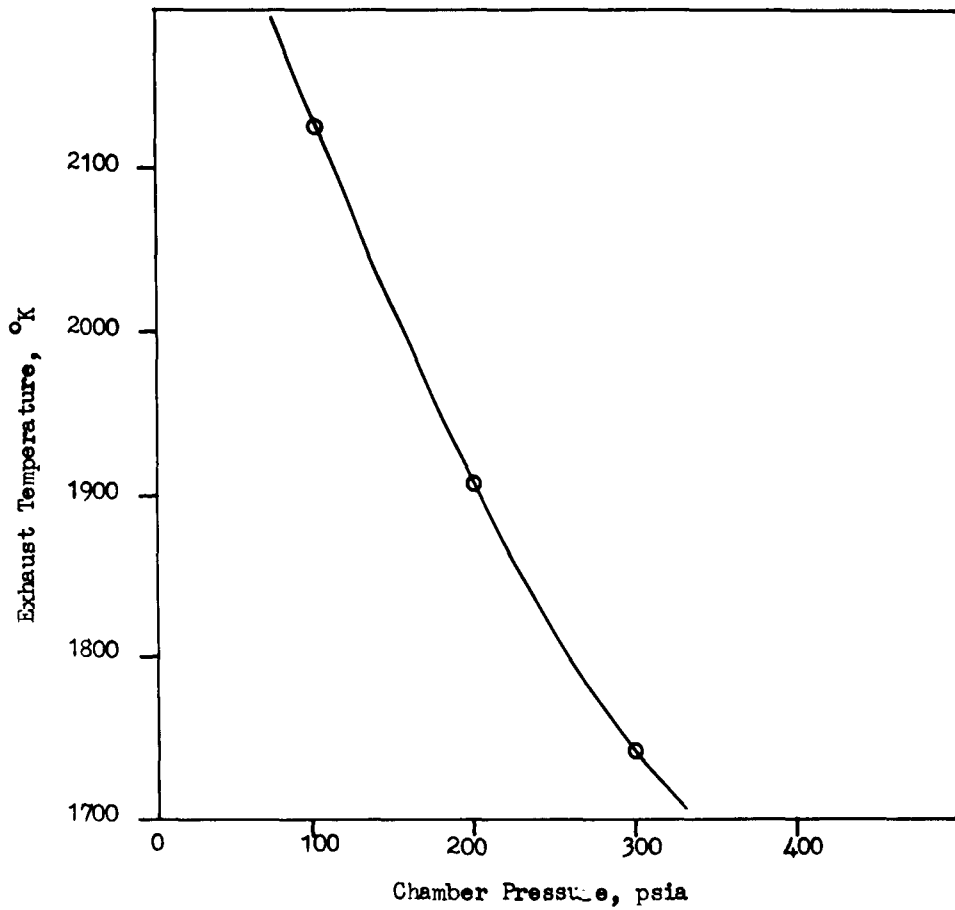


Figure 7. EXHAUST TEMPERATURE VERSUS CHAMBER PRESSURE FOR BF-122 MOD-I

Ambient Pressure: 14.3 psia
Chamber Temperature: 2800°K

TABLE II

CRAWFORD BOMB BURNING RATES FOR

BF-122 MOD-I PROPELLANT

<u>Bomb Pressure (psig)</u>	<u>Burning Rate* (in sec⁻¹)</u>
100	0.173, 0.186
200	0.242, 0.349
300	0.303, 0.277
500	0.379, 0.467

* The pressure exponent measured from the burning rates is 0.51.

TRACERS

Two types of tracers were used. Both introduced the photoemissive element as an inorganic compound, and lithium perchlorate and thallium sulfate were most commonly employed. In many cases the granular salts themselves were used as the tracer material. In other cases the salt was mixed with a polysulfide-epoxy resin. The plastic product was used according to the situation. In strand-burning experiments it was applied to the desired location and allowed to polymerize in situ.

When the polysulfide-epoxy mixture was used in the motor grains it was not convenient to insert it in its uncured state. The mixture was poured into a split mold having a cylindrical cavity. Pressure was then applied in a hydraulic press by means of a mating plunger. The resultant cylindrical tracer strand was removed, sticking being prevented by the use of Poly-Lease 77 mold-release agent (Plastics Division, Allied Chemical Corp., 40 Rector Street, New York 6, N. Y.) and cured overnight in a desiccator. The hard, dense tracer cylinder was finally cut into wafers with a jeweler's saw and these discs were used as the tracer deposits.

The weight composition of the polysulfide-epoxy tracer was as follows:

<u>Amount</u>	<u>Substance</u>	<u>Source</u>
1	tris-dimethylamine methylphenol	DMP-30, Rohm and Haas
10	low mol. wt. liquid polysulfide polymer	LP-33, Thiokol Chemical Corp.
10	epoxy	ERL-2774, Union Carbide Corp.
Variable	tracer salt	
Variable	ammonium perchlorate	

The specific amounts of tracer salt and ammonium perchlorate are given in the experimental portions of this report. In general, when the tracer salt was an oxidizer (e.g. LiClO_4) no ammonium perchlorate was used. The above mixtures were able to sustain self-oxidative combustion, and consequently are propellants. Before use as a tracer each different formulation was subjected to impact and ignition tests. No tendency to detonate was observed.

STRAND EXPERIMENTS

The strand-burning experiments were undertaken to provide a transition between the first year studies of photoemissive materials in gas and uniformly salted propellant flames, and their insertion in discrete locations in operational rocket motors to determine burning rates. Although a burning strand cannot duplicate the temperature, pressure and flow environment of a motor, it is recommended by its economy, and is a suitable experimental medium for conducting preliminary investigations concerning tracer formulation, mode of tracer insertion and the effects of these techniques on the accuracy of the method. The following questions are considered in this section:

1. What is the correlation between tracer signals and events taking place in the propellant.
2. What is the best method for forming a tracer deposit which is completely surrounded by propellant.
3. How reproducible are tracer method burning rates.
4. Do tracer deposits alter the normal burning rate of the propellant.
5. What is the most satisfactory formulation for the photoemissive substance.

Sample Preparation

A cross section through a propellant strand prepared for burning rate studies is shown in Figure 8. The propellant strands that were used in this program were one-quarter inch square. These were cut in measured lengths with a miniature mitre box and knife blade, and the tracer material was inserted into the surface of each piece of propellant. The holes for these deposits were prepared by drilling the cut faces of the propellant blocks. A flat bottom was had by using an end mill, and the depth of the holes were regulated with a drill stop. The 0.24 cm diameter tracer hole constituted 12 per cent of the total strand cross sectional area. These cylindrical holes, whose axes were coincident with the strand axis, were packed with tracer material. The individual pieces were then cemented back together to reform a continuous strand with tracer deposits at known intervals.

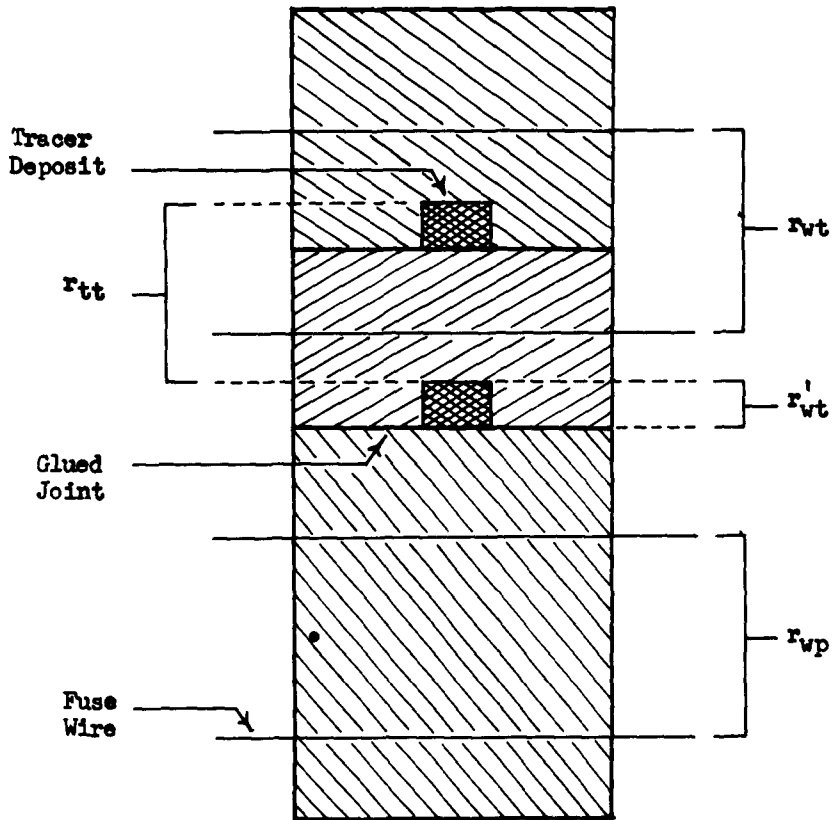


Figure 8. CROSS SECTION OF FUSED STRAND WITH TRACER DEPOSITS

The strands, whose burnt gases were to be spectroscopically examined, were mounted on the strand burner (page 5). To achieve maximum light flux into the spectrometer the entire slit must be filled, but the gas flow from the constantly receding, burning surface of an unconfined strand does not accomplish this satisfactorily. The divergence and dilution of the combustion gases on their upward course decreased the tracer concentration and gas temperature to such an extent that tracer signal could not be detected for tracer deposits that were too far below the optical axis. This problem was met by encasing each strand in an asbestos tube whose mouth was just below the optical axis of the spectroscope. By this means the hot, undiluted gases were delivered to the optimum position without regard to the position of the burning propellant surface.

The first step in treating the tracer containing strand was to inhibit the surface by dipping in asphalt paint. After drying, the strand was tightly rolled in asbestos paper, adhesion being effected with contact cement. Two or three additional layers of wet paper were then bonded on. Good mechanical strength was achieved and no flashing of the flame down the side of the strand occurred.

After the water-soaked asbestos paper had dried fuse wires were sometimes inserted. A drilled template and needle were used to prick the fuse positions into the asbestos covering. The needle, held in a pin vise, was then forced through at each location. A perpendicular relationship between each hole and the strand axis was assured by guiding the needle with a drilled bushing laid on the surface of the strand. With moderate care it was then possible to thread one-half ampere Buss fuse wires through the holes. The purpose of the fuse wires is, of course, to provide burning-time measurements independent from those determined by the tracer signals.

Data Reduction

A typical 35 mm film record from a strand-burning experiment is shown in Figure 9. The terminology used in discussing these data, and formulae for derived quantities are as follows:

$$\begin{aligned} F &= \text{timing mark frequency (sec}^{-1}\text{)} \\ B &= \text{timing marks per unit film length (cm}^{-1}\text{)} \\ r_f &= F/B = \text{rate of film transport (cm sec}^{-1}\text{)} \end{aligned} \quad (1)$$

$$\begin{aligned}
d_f &= \text{distance on film between signals (cm)} \\
d_s &= \text{distance in strand between fuse wires or tracer deposits (cm)} \\
r &= \frac{r_f}{d_f} d_s = \text{burning rate (cm sec}^{-1}\text{)} \quad (2)
\end{aligned}$$

Various burning rates are identified by subscripts. These can be more readily visualized by referring to Figure 8.

$$\begin{aligned}
r_{wp} &= \text{wire method rate for pure propellant} \\
r_{tt} &= \text{tracer method rate for tracer-containing propellant} \\
r_{wt} &= \text{wire method rate for tracer-containing propellant} \\
r_{wt}^v &= \text{wire method rate for portion of strand containing tracer deposit only} \\
r_{wt}^v &= \frac{r_{wp} r_{wt} d_t}{r_{wp} d_s - r_{wt} d_p}, \text{ where} \quad (3)
\end{aligned}$$

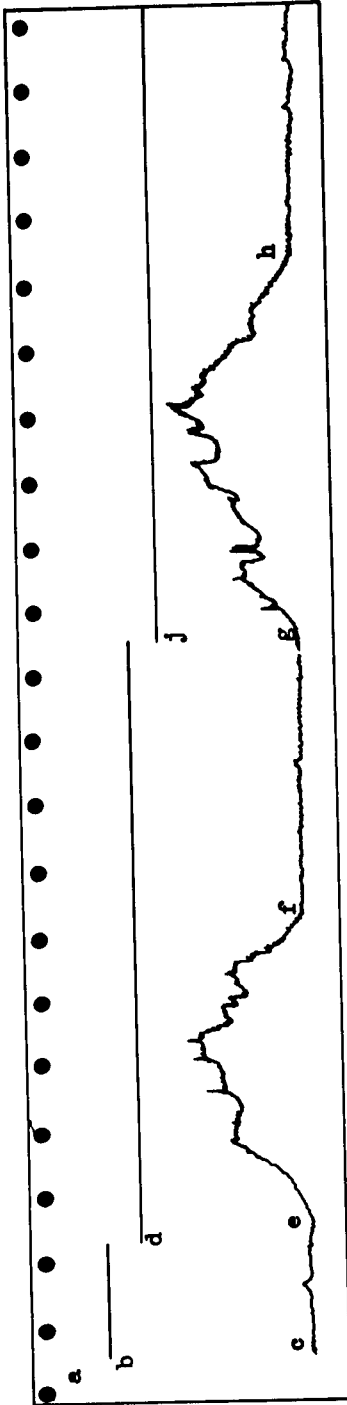
$$\begin{aligned}
d_s &= \text{total distance between the fuse wires} \quad d_t + d_p \\
d_t &= \text{length of tracer deposit} \\
d_p &= \text{length of pure propellant}
\end{aligned}$$

Signal Interpretation

There are various possible ways in which the tracer signals can be used to find burning rates. A rate can be found by using the time duration of signal from a single deposit. This is the interval e-f in Figure 9 on page 21. Rates can also be found from signals originating from two deposits. The time intervals for this method could be, for example, e-g, f-g or f-h. The appropriate strand length must, of course, be associated with each of these time intervals to find the burning rate.

Some examples of burning rates derived from these different time intervals are given in Table III, where they are compared to the fuse-wire rate for a propellant strand which contained no tracer material. These strands were not all cut from the same length of propellant, and it was later found that rate differences can be expected under such circumstances. The variations found in Table III, however, are much larger than normally arise from this cause.

It is apparent that tracer-method burning rates found from the time interval between the end of one signal and the beginning of the next are too large (Strand 18), while use of the time interval for a single signal (Strand 23) gives a rate which is too small. These opposite results indicate that both errors cannot be primarily connected with any effect of the



Time →

- a. Timing marks from Fairchild electronic film control
- b. Fuse-circuit voltage trace
- c. Background photomultiplier trace
- d. First fuse wire severed
- e. Signal from first tracer deposit
- f. End of tracer signal
- g. Signal from second tracer deposit
- h. End of tracer signal
- j. Second fuse wire severed

Figure 9. TYPICAL STRAND BURNING RECORD ON 35 MM FILM

tracer on the actual burning rate, but rather that some of the error must arise from misinterpretation of the data. The causative phenomenon, common to both cases, is that the inorganic tracer salt is not gasified at a rate equal to the rate with which the surrounding organic material is burned away. Thus, after strand burning has progressed over a length equal to the depth of the tracer deposit, some salt still remains. This continues to recede with the solid-propellant surface, and the last signal from a tracer deposit is received from a position below that of its original place of incorporation.

The result is that the time interval between the end of one signal and the beginning of the next actually pertains to a distance which is smaller than the interdeposit distance which obtained when the strand was originally prepared. The burning rate, calculated, of course, from the latter distance is then too large. Conversely, the time interval over which a single signal lasts actually pertains to a larger propellant distance than indicated by the original depth of the tracer deposit, and the calculated burning rate is too small.

It is evident that both of these errors can be avoided by not using the end of a tracer signal as a time reference. • Thus, it is necessary to determine time intervals from the onset of signals which arise from two consecutive tracer deposits. The burning rates for Strands 27 - '32 in Table III were determined in this manner, and any discrepancy between these values

$$r_{tt} = 0.110 \pm .002 (24)$$

and that found by fuse-wire method

$$r_{wp} = 0.102 (2)$$

must be attributed to a different cause. There are three possibilities - the difference represents a real difference in the propellant samples; the tracer deposits are actually changing the burning rate; or a systematic error exists.

These matters will be returned to after the following section.

TABLE III

TRACER METHOD BURNING RATES

<u>Strand</u>	<u>Signal Type</u>	<u>Tracer Composition (by weight)</u>	<u>Burning Rate (cm sec⁻¹)</u>
1	Fuse-wire	No tracer deposits	0.102 (2)*
18	f-g	LiClO ₄ + PE**	0.132 ± .008 (4)
23	e-f	LiClO ₄	0.091 (1)
27	e-g	LiClO ₄ + PE	0.107 ± .003 (4)
28	e-g	LiClO ₄ + PE	0.108 ± .002 (4)
29	e-g	LiClO ₄	0.110 ± .001 (4)
30	e-g	LiClO ₄	0.1095 ± .0004 (4)
31	e-g	LiClO ₄ + 2PE + AP***	0.113 ± .001 (4)
32	e-g	LiClO ₄ + 2PE + AP	0.113 ± .004 (4)

* Numbers in parentheses indicate number of replicates

** Polysulfide-epoxy resin

*** Ammonium perchlorate

Signal Duration

The fact that signal is received from a tracer deposit for a longer time than the propellant takes to burn the same distance puts a limit on the minimum spacing between consecutive tracer deposits. Signals from deposits placed any closer than this minimum will overlap and in effect act as a single tracer. The average signal duration, indicated e-f and g-h in Figure 9, for Strands 27-29 is 3.07 ± 0.54 seconds. This time, multiplied by the burning rate, yields $0.34 \pm .06$ cm which is the effective thickness of a single deposit, and is the minimum allowable separation between deposits. The effective thickness is approximately twice the true thickness of these deposits, namely 0.20 centimeters.

It is possible that signal duration increases with increasing tracer thickness. A tracer deposit should, however, be as thin as mechanical considerations allow, and since no need for deposits thicker than 0.2 cm was anticipated, further experiments in this vein were not conducted.

Temperature Effect

The possibility of further systematic errors, beyond those involved in signal interpretation, was examined by comparing tracer-method rates with fuse-wire rates. The rates that were determined were r_{wt} and r_{tt} , which are identified in Figure 8, page 18. The strand environment over which both rates were determined was the same. In both cases the burning surface traversed one tracer deposit and equal amounts of pure propellant. Thus, any alteration of the burning rate caused by a tracer deposit must appear equally in both r_{wt} and r_{tt} . It follows, that any discrepancy between these rates can only result from the method of interpreting the data, and cannot result from any alteration of the properties of the propellant.

The results of these experiments, reported in Table IV, yield the average values

$$\begin{aligned} r_{tt} &= 0.096 \pm .002 \text{ (10)} \\ r_{wt} &= 0.100 \pm .002 \text{ (9)} \end{aligned}$$

Whether this 4 per cent discrepancy arises from random errors or a systematic error in the tracer method can be determined statistically by means of Gosset's t-test⁴, which yields

$$t = 2.8, \text{ 16 degrees of freedom}$$

4. H. Cramer, The Elements of Probability Theory, John Wiley & Sons, New York, 1955, Chapter 15.

as compared to the critical t - values for the 1 per cent and 5 per cent probability levels

$$\begin{aligned}t &= 2.9, \text{ 1\% probability} \\t &= 2.1, \text{ 5\% probability}\end{aligned}$$

It is seen that there is considerably less than a 5 per cent chance that the average difference in burning rates arose from random errors.

Thus, in order to explain the low value of r_{tt} it is necessary to find some phenomenon which systematically makes the measured burning time, as found from the tracer signals, too large. Such an explanation can be based on what is termed the tracer time-lag. When the burning surface reaches a tracer deposit a certain amount of time elapses before the presence of tracer signal can be recognized. If this time-lag is the same for two successive tracer deposits the tracer rate, r_{tt} , will equal the fuse-wire rate, r_{wt} . However, if the time-lag, t , is not the same for both deposits the tracer rate will be falsified, as can be seen from the following expression

$$r_{tt} = \frac{d_s}{t} = \frac{d_s}{(T_2 + t_2) - (T_1 + t_1)}$$

where T_2 and T_1 indicate the actual times of arrival of the flame front at each deposit. More specifically, if $t_2 - t_1$ is positive, the burning rate will be too small, and t must increase with each successive tracer deposit to give this result.

The reason t continuously increases is probably related to exhaust-gas cooling, which becomes progressively larger as the distance of the tracer deposit from the mouth of the asbestos tube which contains the strand increases. This progressive cooling is evidenced by a progressive decrease in signal intensity, and the onset of a weak signal is not so apparent as the onset of a stronger one.

This type of systematic error in the tracer method is not peculiar to strand rates. A rocket which does not have a neutral burning characteristic will also undergo temperature changes in its exhaust. Then, burning rates, as indicated by the tracer method, will be expected to be too small or too large according to whether the exhaust temperature is dropping or rising.

TABLE IV

COMPARISON OF TRACER AND FUSE WIRE BURNING RATES
FOR THE SAME ENVIRONMENT

<u>Strand</u>	<u>Signal*</u>	<u>r_{wt}</u> (cm sec ⁻¹)	<u>r_{tt}</u>
39	1	.0947	.0954
	2	.0993	.0983
	3	.1049	.0898
	4		
40	1	.1011	.0960
	2	.1076	.0955
	3	.0996	.0969
	4		
41	1	.0978	.0998
	2	1.000	.0958
	3	.0980	.0964
	4		
		<u> </u>	<u> </u>
		$\bar{r} = .100 \pm .002$	$\bar{r} = .096 \pm .002$

* The fuse wires and tracer deposits are numbered consecutively from top to bottom in the strand

Effect of Tracer Deposits

The following experiments compare wire-method burning rates for pure propellant and propellant which contained tracer deposits. Composition variations, previously mentioned, were minimized by using a single, stock-piece of propellant to compare both rates for any set of data. The use of the fuse-wire method to find both rates eliminates the systematic error which arises from the tracer time-lag. Thus, any discrepancy between these rates reflects a real modification of the propellant by the tracer deposit.

Formation of a tracer deposit requires both the insertion of tracer material and the introduction of a cemented interface, as described on page 17, and either or both of these can affect the burning rate.

The effects of cemented interfaces were examined by determining wire-method burning rates for lengths of propellant which had an interface between each pair of fuse wires. The burning rates are given in Table V. It was previously found that contact cement acted as an inhibitor and sometimes caused extinguishment, but it can be seen that the average rates for both Duco cement mixed with ammonium perchlorate ($\bar{r} = 0.108$) and plain Duco ($\bar{r} = 0.110$) agree with the rate for pure propellant ($\bar{r} = 0.109$) within the experimental error. Duco cement was used to form the interfaces in all of the following experiments.

The effects of tracer materials were found by determining the wire-method burning rate only over the length of strand which actually contained the tracer deposit. To exaggerate any perturbations a 1 cm deposit length was used. The most desirable experimental arrangement would be to insert the fuse wires coincident with the extremities of the tracer. However, as reference to Figure 8, page 18 shows, this would require one wire to pass through a glued interface, and it was feared that this joint might be disrupted. Accordingly, the fuse wires were placed as in Figure 8, beyond the ends of the tracer deposit. Such a rate, r_{wt} , therefore includes the burning rate of pure propellant as well as that for the tracer-containing section of the strand. The rate for the latter, r_{wt} , may be extracted by equation (3), page 20. The results are given in Table VI.

TABLE V

EFFECT OF CEMENTED INTERFACES ON THE BURNING RATE

<u>Strands</u>	<u>Interface</u>	<u>Burning Rate</u> <u>(cm sec⁻¹)</u>
64-67	None	.109 ± .002 (3)
	Duco	.1121 ± .0004 (3)
	Duco	.110 ± .003 (3)
	Duco	.1091 ± .0008 (3)
72-74	None	.109 ± .003 (3)
	Duco ± AP*	.106 ± .001 (3)
	Duco ± AP	.1078 ± .00002 (2)
	Duco ± AP	.109 ± .002 (4)

* Ammonium Perchlorate

TABLE VI

EFFECT OF LITHIUM PERCHLORATE ON THE BURNING RATE

<u>Strand</u>	<u>Tracer Depth (cm)</u>	<u>Burning Rates (cm sec⁻¹)</u>		<u>Error (%)</u>
		<u>r_{wt}</u> (includes tracer)	<u>r_{wp}</u> (propellant only)	
38	1.0	.091 (1)	.106 ± .006 (2)	-14
43-47	1.0	.100 ± .001 (3)	.1060 ± .0005 (3)	-6
48-52	1.0	.095 ± .001 (4)	.108 ± .002 (3)	-12
		<u>r_{wt}</u>	<u>r_{wp}</u>	
75-77	0.1	.102 ± .002 (11)	.103 ± .004 (2)	-1

It can be seen that the average decrease in the burning rate is ten per cent over a deposit length of one centimeter. Thus, if no other errors are present, the ratio of a tracer-method rate, r_{tt} , to the true burning rate, r_{wp} , can be represented

$$\frac{r_{tt}}{r_{wp}} = \frac{d_p + 0.9 d_t}{d_s}$$

where d_s is the total distance between the tracer deposits, d_t is the thickness of one deposit, and d_p is the remaining distance, composed of pure propellant. This expression can be used to determine the accuracy which is possible with the tracer method. For example, if any accuracy of one per cent is desired for burning rates which have a one centimeter spatial resolution, then $d_p = 1 - d_t$, and

$$\frac{r_{tt}}{r_{wp}} = 0.99 = \frac{1.0 - 0.1 d_t}{1.0} \quad (4)$$

which yields $d_t = 0.1$ cm as the maximum permissible thickness of each tracer deposit.

Strands 75-77 (the last entry in Table VI) were prepared in this manner, and it can be seen that the average burning rate, r_{wt} , agrees with the true rate, r_{wp} , within the experimental error.

Signal Intensity

Various tracer compositions were used in the strand-burning experiments. It was hoped that the polysulfide-epoxy formulations, which are themselves propellants, would effect a more rapid and complete vaporization of the photoemissive salt. The 35 mm film records showed, however, that there were no significant differences in signal intensity or signal duration between pure salt and polysulfide-epoxy tracers.

Recommended Procedure

The results of the strand-burning experiments can be summarized as a recommended procedure for validating the use of any particular tracer-propellant combination. It is understood, in the following, that all rate comparisons are made within experiments conducted on strands originating from a single parent piece of propellant. This stipulation is indicated by the considerable differences that have been found between different propellant batches.

1. Construct a strand which only contains cemented interfaces. Confirm, by comparison of its burning rate with that for pure propellant, that the chosen cement is suitable.
2. Construct a strand with a long tracer deposit. Find the wire-method rate only over the length of the deposit. This rate has previously been identified as r_{wt}' .
3. If r_{wt}' differs significantly from the rate for pure propellant, r_{wp} , use these values to find the fractional error, x , which a short tracer deposit would introduce into the burning rate of a longer piece of propellant:

$$x = 1 - \frac{d_p + d_t (r_{wp} - r_{wt}')}{d_s r_{wp}} \quad (4a)$$

4. Manipulate the distance between the tracer deposits, $d_s = d_p + d_t$, and the deposit thickness, d_t , to yield the desired minimum error, x .
5. Construct a strand in accord with the results of (4) and compare r_{tt} , r_{wp} , r_{wt} . Find r_{tt} by using the initial signal from two consecutive tracer deposits as the time markers. Agreement between r_{wt} and r_{wp} within the desired limits confirms the results of (3) and (4). Comparison of r_{tt} and r_{wt} reveals if there is any systematic error in the tracer method. Temperature effects (page 29) should be eliminated in this test by using a larger strand cross section than was employed for this work.
6. When the tracer method is applied to the determination of motor burning rates it may be found that successive tracer signals differ considerably in rate-of-rise and/or intensity for intervals of rapid pressure change (the temperature effect). Be prepared to regard these rates with scepticism.

MOTOR BURNING RATES

Tracer Insertion

A motor grain containing two tracer deposits in one location is shown in Figure 6, page 11. When tracer is inserted in more than one location a different tracer salt is used for each. The different characteristic frequencies associated with each tracer serves to identify the location from which the signal arose. Thus, the number of possible data points in the engine is limited only by the number of suitable tracer materials. The demonstration of the technique, however, does not require more than one location, and no test was made with more than two.

The number of deposits (i.e. the distance between deposits) in a single location is limited by the accuracy considerations described by equation (4a), page 31, and a one-centimeter spacing was used in all cases.

The tracer holes in the motor grain were formed by drilling. The diameter of these holes equalled that of the grain center-perforation (0.5 in), and their cross sectional area was 0.7 per cent of the total burning area (28.1 in²). The grains are cast inside a cardboard tube whose inner surface is coated with inhibitor. The elastic inhibitor layer tends to close up after the drilling operation and reduces the diameter at that point. To prevent this, a thin walled bushing with saw teeth ground into one end was slipped on the drill. It was locked in such a position that when the drill reached the desired depth the saw teeth just penetrated the inhibitor thickness. Thus, the hole in the propellant was maintained at the desired diameter while the hole through the tube-inhibitor layer was sufficiently enlarged to account for inhibitor elasticity. After drilling, the hole was bottomed with an end mill, and the depth determined with a depth gauge.

The individual tracer deposits were separated by plugs of propellant. These were formed with a cork borer. It was found that pressing the borer through the propellant at a deliberate pace, without twisting, resulted in smooth cylinders of uniform diameter. A few motor grains were reserved for making these plugs. It is not advisable to cast a propellant slab especially for this purpose, since different geometries cure differently when subjected to the same treatment cycle, and burning rate differences between the plugs and the motor grains will result.

Two kinds of tracer deposit were used. Initially, the tracer was inserted in the form of loose salt, with individual deposits separated by cylinders of propellant. It was found, as will be described later, that these porous deposits perturbed the normal burning of the motor grain, and their use was abandoned.

The other kind of deposit, which proved to be completely satisfactory, was made from pressed cylinders of polysulfide-epoxy bonded tracer salt. The preparation of this type tracer is described on Page 18. Discs about 1 mm thick were cut from this cylinder. The tracer discs were alternated with 1 cm cylinders of propellant, adhesion being effected with Duco cement, to form a round tracer-containing strand. A small amount of Duco was poured into the drilled grain hole and the glue-smearred strand inserted. Trapped air and excess glue escaped via a shallow notch previously cut along the strand length.

The motor grain was supported by a rod through its center perforation when the tracer strand was inserted. This allowed the strand to be forcefully bottomed in the drilled hole without distorting the inner grain surface. After the glue had dried the excess strand length was trimmed flush with the outer surface of the cardboard grain tube. This exposed propellant surface was then inhibited with three patches of asbestos paper, successively applied with contact cement.

Firing Procedure

The ignition circuit for the rocket motor is shown in Figure 5, page 10. The following sequence was followed.

1. Close line switch S_1 (key operated).
2. Close toggle switch S_2 which energizes relay R_1 to close contact R-1. This function duplicates the line switch and is included as a safety measure.
3. Close switch S_3 to energize relay R_2 which operates the four R-2 contacts. This operation removes the squib terminals from ground potential in preparation for a continuity check.
4. Press pushbutton switch S_5 and ascertain continuity with microammeter (voltmeter plus 2K resistor).
5. Turn on Fairchild camera for recording tracer signals.
Turn on CEC oscillograph for recording motor pressure.

6. Close fire switch S_4 to energize relay R_3 , closing both R_3 contacts. This also simultaneously applies a voltage to the time coordinate of the pressure recorder and turns on the timing light in the Fairchild camera. Thus the time scales of the pressure curve and of the tracer signals can be synchronized.

Data Reduction

The tracer signals from the motor firings were recorded and interpreted in the same manner as described for the strand experiments. A typical data record, excepting the fuse-wire signals, is depicted by Figure 9, page 21.

In addition to tracer signals, the motor pressure was also recorded. An example is shown in Figure 10. The step in the time coordinate, at t_0 , marks the closing of the firing switch. The latter operation also initiates the time markers on the tracer film record, Figure 9. Immediately after t_0 the pressure spike from the squib is seen, and the pressure minimum which demarcates the squib pressure drop from the rise associated with the motor grain was considered to be the moment when grain burning was initiated.

This point t_0 , was used as a time marker in conjunction with the signal from the first tracer deposit to determine an initial burning rate that could not be found from tracer signals alone. To determine the initial rate by the tracer method requires that the first tracer deposit be flush with the inner grain surface. While this can readily be done, it was found that tracer signal from such a deposit was obscured by the broad-band radiation pulse that occurs upon squib ignition.

Burning rates, being determined over finite time intervals, are average values, and it is necessary to associate each rate with the average motor pressure for the same time interval. This average pressure is defined

$$\bar{p} = \frac{\sum P \Delta t}{\sum \Delta t} \quad (5)$$

The pressure curve was divided into intervals, Δt , sufficiently short that the pressure over each interval could be considered a straight line, and the median pressure for each interval was taken as P in equation (5).

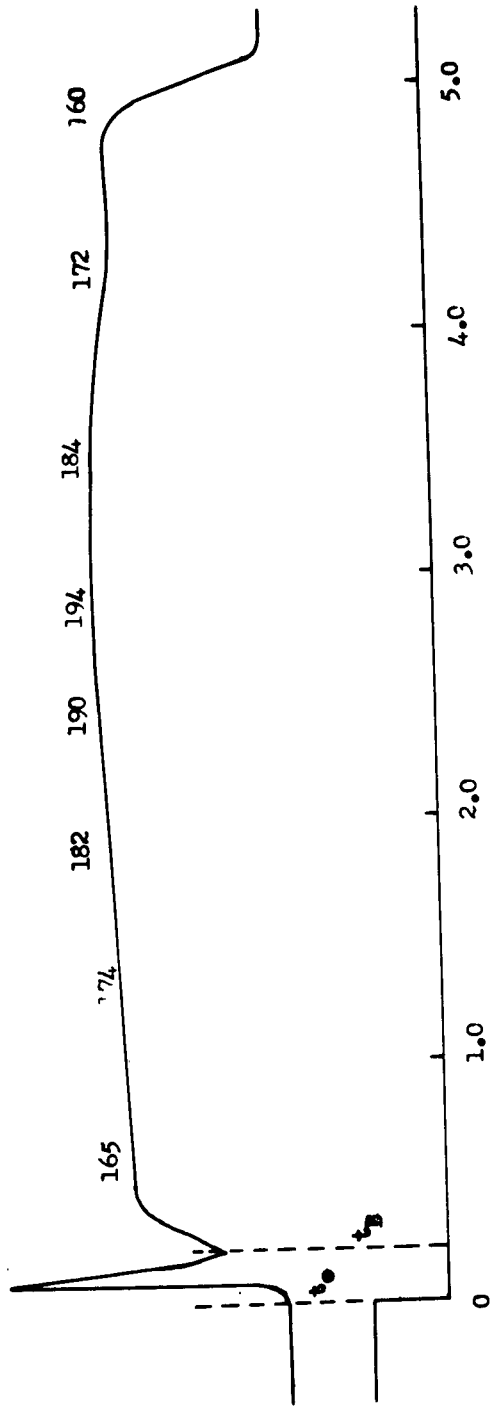


Figure 10. MOTOR PRESSURE TRACE

Any variation in burning characteristics between grains will be reflected by variation in their pressure curves. The variation (i.e. error) of an individual motor run is best expressed in terms of the difference between the area underneath its pressure curve and the area underneath an average pressure curve. This difference must be found on a point-by-point basis, since it is possible for two widely different curves to encompass the same total area. Specifically, a correlation function for the j-th pressure curve is defined

$$C_j = \frac{\sum_{i=1}^m \bar{P}_i \Delta t_i - \sum_{i=1}^m |\bar{P}_i - P_i^j| \Delta t_i}{\sum_{i=1}^m \bar{P}_i \Delta t_i} \quad (6)$$

where $i = 1, 2 \dots m$

is the number of time intervals, Δt , into which the curve has been divided, and

$$\bar{P}_i = \frac{1}{n} \sum_{j=1}^n P_i^j \quad (7)$$

is the average of the $j = 1, 2 \dots n$ pressure curves for the i-th time interval. Accordingly, the first term in the numerator is the total area underneath the average pressure curve, and the second term is the sum of the absolute area differences, for each time interval, between the average curve and the j-th curve whose correlation is being found. Thus, the better the fit of curve - j with the average curve, the closer C_j will approach unity.

Spectrometer Aperture

The first motor grain contained lithium perchlorate and thallium sulfate tracer deposits, but no signal was received on either channel, indicating that a higher instrument sensitivity than was used for the strand experiments was required. There are two reasons for this. The motor had only 1 per cent area-ratio of tracer to propellant, while the tracer constituted 12 per cent of the burning surface in the strand experiments. Furthermore, the expanded motor exhaust was much cooler than the burnt gases from the unconfined strands.

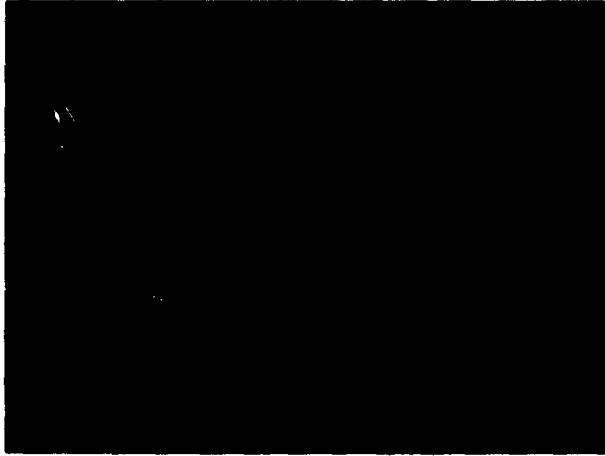
The 25-micron spectrometer entrance slit was replaced with a 100-micron one, and the 100-micron exit slits were removed entirely. This theoretically increases the light flux by a factor of sixteen. In actuality, signal levels from test sources (a lithium salted flame and an Osram thallium lamp) increased from about 50 millivolts to 35 volts for both emission lines. Since the scattered light contribution from one source to the other photomultiplier channel was only 5 millivolts, the 700-fold signal increase indicated that the original exit slits were not aligned to give optimum sensitivity.

Perfect alignment of exit slits with an instrument of such high dispersion is a very tedious process. Moreover spectral lines at the exit plane have a slight curvature and a straight exit slit will not give optimum conditions. Consequently, it was decided to achieve the required signal level by retaining the enlarged slits, rather than attempt a more refined adjustment of the original ones.

Background Radiation

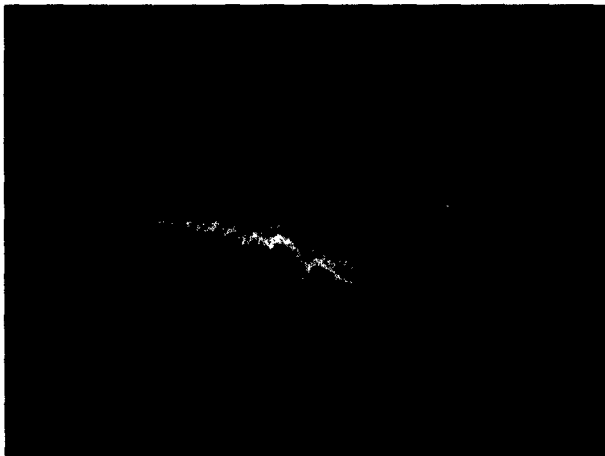
Another result of increasing the aperture of a spectrometer is to degrade the spectral purity if background radiation is superimposed on the discrete spectral lines. This effects a decrease in the signal-to-noise ratio. The intensity of background radiation was found by firing a blank grain (i.e. one without tracer deposits). A one-tenth volt spike (Figure 11) followed by a continuous noise signal which rose to about 0.1 volt intensity at motor burnout was measured (Figure 12), as compared to the fact that no background was previously detected in the strand experiments when the spectrometer had its smaller aperture.

This background originates from both the motor squib and the propellant itself. Two kinds of squibs, pyrotechnic and black powder, were ignited in a dummy motor grain (a grain formulated without oxidizer). Both of these caused large signal spikes in the lithium and thallium channels, lasting for as long as 0.5 second, with the most intense signal arising from the pyrotechnic squib. The emanation of background signal from the propellant itself was established by the large signal which resulted when a propellant strand, which could be set ablaze without the use of a squib, was used as the light source.



Time = 1.0 sec/cm Sensitivity = 50 mv/cm

Figure 11. RADIATION FROM MOTOR SQUIB



Time = 0.5 sec/cm Sensitivity = 50 mv/cm

Figure 12. RADIATION FROM MOTOR GRAIN

It is not surprising to find such radiation from a metallized pyrotechnic squib, or even from the black powder one, since it was ignited with a hot wire. The propellant, however, contained only 0.25 percent magnesium oxide as its sole solid constituent, and this seems to be the only possible source of continuum radiation.

Signal Detection

The background radiation caused some difficulty in detecting the tracer signals. Before discussing this problem it is necessary to make some comments about the signal in the absence of background radiation.

The strand experiments, where the smaller slits made the background negligible, showed that the tracer signal consisted of a DC component on which considerable noise was superimposed (Figure 9, page 21). Both of these components proved to be of value in detecting the onset of tracer signal. In most cases a rapid rise of the DC signal was had, and the intersection of its slope with the base-line indicated the onset of signal. At other times, however, the liberation of tracer was apparently more erratic and the initial slope could not readily be defined. In these cases the onset of noise from the photomultiplier tube served to fix the point at which tracer signal first began. The high background signal in the motor tests eliminated this second method for identifying tracer signal and degraded the first.

As described in the preceding section, the average background level was about 0.1 volt, and this necessitated using a full-scale sensitivity of one volt so that ample recording room for the tracer signal was available. In comparison, the full-scale sensitivity in the strand work was only 0.1 volt. The increased setting used in the motor work greatly reduced the slope of the initial tracer signal, and the onset of signal could not be so readily identified. The fact that the background signal also has noise superimposed on it eliminated the alternate method, the use of tracer signal noise, as a means for identifying the onset of signal.

The presence of background noise introduces a further consideration which can affect the accuracy with which tracer signal is located. The decreased slope of the DC signal component, occasioned by the required decrease in sensitivity, can be counteracted by decreasing the recording speed. There is, however a limit to this recourse, apart from any resultant decrease in accuracy of linear measurements made on the

film record. If the recording speed is sufficiently lowered, the DC component of the tracer signal is so compressed in time that it is indistinguishable from a noise spike.

It was noticed that the rate of signal rise was much slower in the motor tests than it was in the strand experiments. This is probably related to differences in tracer deposit configuration. In the strand experiments both the burning surface and the tracer deposits were planar, and the entire tracer area was exposed to the flame at one instant. In the motor tests the tracer deposits were also planar, but the burning surface was cylindrical. Thus the initial contact of the flame with the deposit was limited to the cylinder-plane tangent. No attempts to make the tracer surface conform to that of the burning surface were made.

Motor Pressure

The first motor tests used loose, granular salt to form the tracer deposits. It was found that small steps in the motor pressure occurred with this type deposit. These pressure steps correlated quite well with the tracer appearance time, and it was concluded that the propellant flame was flashing into the small, cylindrical cavities which contained the porous tracer. This was corrected by using the dense, pressed polysulfide-epoxy tracer formulation.

It was still possible that the tracer deposits were altering the normal burning characteristic of the motor grain in a manner that could not be so obviously perceived. To reveal any such effects the correlation function, CJ , described by equation (6), page 36 was used. The pressure traces from two blank grains were averaged to form a reference curve. The correlation between these two curves was $C = 0.88$. The pressure curves of two tracer-containing grains were then compared to the reference curve to yield correlations of $C = 0.92$ and 0.94 . These grains each had two tracer deposits, and the excellent correlations were taken as an indication that the pressed tracer deposits did not change the normal burning of the motor.

Burning Rates

The experimentally determined motor burning rates are summarized in Table VII. All of these pertain to the head-end of the tubulated portion of the grain. Consequently, they should be free of any erosive component. The rate indicated r_1 was found by using the motor ignition time, t_B , as one time marker, and the first tracer signal as the second time marker. The rate indicated r_2 was determined between the two tracer deposits.

TABLE VII

TRACER METHOD ENGINE BURNING RATES

Run*	Burning Rates (cm/sec) and Pressures (psig)			
	r_1	\bar{P}_1	r_2	P_2
E21	.722	203	.462	195
E22	.628	190	.436	199
E23	.462	200	.460	198
E24	.464	201	.492	203
E25	.550	201	.490	200
	$.56 \pm .09$	199 ± 4	$.47 \pm .02$	199 ± 2
E33	.396	145	.430	166
E34	.376	144	.428	160
E35	.404	124	.344	160
E36	.368	161	.565	172
E42	.437	154	.468	172
E43	.424	148	.464	156
	$.40 \pm .02$	146 ± 8	$.45 \pm .05$	164 ± 6

* Runs E21-E25 used granular LiClO_4 and $\text{Ti}_2(\text{SO}_4)_3$ tracer deposits. The rest of the runs used pressed polysulfide-epoxy tracers.

The pressures are average values as defined by equation (5), page 34. The first group of runs, E21 - E25, used granular salt tracers, and the rest used the pressed polysulfide-epoxy formulation. The larger average pressure for the first group of runs is apparent. As discussed above, it is believed that this was caused by flame penetrating the granular salt deposits and igniting the inside of the tracer holes.

The rates r_1 , which used t_B as the initial time point, are suspect, since this manner of defining the moment of grain ignition is somewhat arbitrary. It must also be pointed out that \bar{P}_1 cannot be used to determine the functional relationship between the burning rate and pressure. The reason for this is that \bar{P}_1 pertains to a portion of the motor operation where a large pressure gradient occurs. An average burning rate over a region of pressure change can be expressed in terms of the individual rates along this path:

$$r = cP^a = \frac{c \sum_{i=1}^n P_i^a}{n} \quad (8)$$

where n is the number of equal time intervals into which the total time has been divided. The question is - what are the relationships between P , the actual pressures P_i to which the propellant has been subjected, and the average pressure, \bar{P} , defined by equation (5), page 34. These relationships are

$$P = \left[\frac{\sum P_i^a}{n} \right]^{1/a} \neq \bar{P} = \frac{\sum P_i}{n} \quad (9)$$

Not only is P not equal to \bar{P} , but it can be readily shown that the relationship between them is not necessarily monotonic. Thus, average burning rates are not well suited for defining burning rate relationships.

These comments do not pertain so strongly to r_2 and \bar{P}_2 , since the pressure variation was quite small when this rate was being determined. However, values of r_2 and \bar{P}_2 did not exhibit enough variation to warrant their use for purposes of finding the rate parameters c and a in equation (8).

Discussion

The tracer method, as applied to motor burning rates, has two principal weaknesses (1) The low signal-to-background ratio, which varied between five and ten, and (2) The slow rate-of-rise of the tracer signal.

Attempts were made to enhance the signal strength by exciting the exhaust gases with a high-voltage spark. Although this was fairly satisfactory when applied to strands, problems in maintaining the positional stability of the discharge were encountered, and the spark image could only be kept focused on the entrance slit with difficulty. Since this condition would be aggravated in a high-velocity stream the application of this technique to the motor runs was not attempted.

Another approach to increasing the signal-to-background ratio is to reduce the background. An extra photomultiplier tube was installed next to the tracer tube. Since the former would receive only background signal, the difference between its output and the tracer tube output should consist only of tracer signal. This method of canceling background radiation was attempted on several motor runs by feeding the two tube outputs into a differential amplifier. The results were ambiguous and no conclusions could be made.

The second problem, low rise rate of the tracer signal was principally caused by the difference in surface geometries between the tracer deposit and the motor grain. The first exposure of tracer is only along their line of contact, and only after this does the burning surface uncover the full area of the tracer deposit. This problem was contributed to by the necessity of using the pressed tracer deposits, since they did not give signal intensity equal to that for the granular ones. This is the principal reason for the better precision of the first group of burning rates in Table VII, page 41. It would no doubt be possible, if troublesome, to improve this situation by making tracer deposits of the same surface configuration as the burning surface of the motor grain.

That the above difficulties are not overly serious is demonstrated by the reasonable precision with which motor burning rates were determined, and the tracer method can be recommended as a useful diagnostic method for examining rocket motor malfunctions.

<p>Office of Research Analyses Office of Aerospace Research Holloman AFB, New Mexico</p> <p>STUDY OF TRACER METHOD FOR SOLID PROPELLANTS, February 1963. viii + 42 pp, including illustrations and tables. (ORA-63-3) unclassified report</p> <p>A photometric method for determining local burning rates in solid propellant motors is described. Metallic salt-polymer mixtures (tracers) are inserted in known locations in the motor. Resonant radiation from the vaporized metal provides light pulses (over)</p> <p>in the motor exhaust. Spectrographic time resolution of these pulses and the known distances between deposits in the grain yield the burning rates. Preliminary strand experiments are used to estimate burning rates of tracer and propellant under engine conditions. These values are introduced in an expression relating accuracy of photometric burning rate to tracer thickness, separation between tracer deposits, and tracer and propellant burning rates. Tracer thickness and separation in the test engine for a desired accuracy are thus defined. Engine burning rates reproducible to +7 per cent for a one centimeter separation were easily obtained.</p>	<p>UNCLASSIFIED</p> <p>1. Solid, Rocket, Propellants. 2. Burning Rate 3. Spectroscopy 4. Test Methods</p> <p>I. Contract No. AF29(600)-3020 II. Reaction Motors Div., Thiokol Chemical Corp., Denville, N.J. III. D. Fleischer</p> <p>UNCLASSIFIED</p>	<p>Office of Research Analyses Office of Aerospace Research Holloman AFB, New Mexico</p> <p>STUDY OF TRACER METHOD FOR SOLID PROPELLANTS, February 1963. viii + 42 pp, including illustrations and tables. (ORA-63-3) unclassified report</p> <p>A photometric method for determining local burning rates in solid propellant motors is described. Metallic salt-polymer mixtures (tracers) are inserted in known locations in the motor. Resonant radiation from the vaporized metal provides light pulses (over)</p> <p>in the motor exhaust. Spectrographic time resolution of these pulses and the known distances between deposits in the grain yield the burning rates. Preliminary strand experiments are used to estimate burning rates of tracer and propellant under engine conditions. These values are introduced in an expression relating accuracy of photometric burning rate to tracer thickness, separation between tracer deposits, and tracer and propellant burning rates. Tracer thickness and separation in the test engine for a desired accuracy are thus defined. Engine burning rates reproducible to +7 per cent for a one centimeter separation were easily obtained.</p>	<p>UNCLASSIFIED</p> <p>1. Solid, Rocket, Propellants. 2. Burning Rate 3. Spectroscopy 4. Test Methods</p> <p>I. Contract No. AF29(600)-3020 II. Reaction Motors Div., Thiokol Chemical Corp., Denville, N.J. III. D. Fleischer</p> <p>UNCLASSIFIED</p>
---	--	---	--